LAWRENCE
LIVERMORE
NATIONAL
LABORATORY

LLNL-CONF-691080

LLNL Laser-Compton X-ray Characterization

Y. Hwang, T. Tajima, G. Anderson, D. Gibson, R. Marsh, C. Barty

May 5, 2016

7th International Particle Accelerator Conference
Busan, South Korea
May 8, 2016 through May 13, 2016

Disclaimer

This document was prepared as an account of work sponsored by an agency of the United States government. Neither the United States government nor Lawrence Livermore National Security, LLC, nor any of their employees makes any warranty, expressed or implied, or assumes any legal liability or responsibility for the accuracy, completeness, or usefulness of any information, apparatus, product, or process disclosed, or represents that its use would not infringe privately owned rights. Reference herein to any specific commercial product, process, or service by trade name, trademark, manufacturer, or otherwise does not necessarily constitute or imply its endorsement, recommendation, or favoring by the United States government or Lawrence Livermore National Security, LLC. The views and opinions of authors expressed herein do not necessarily state or reflect those of the United States government or Lawrence Livermore National Security, LLC, and shall not be used for advertising or product endorsement purposes.

LLNL LASER-COMPTON X-RAY CHARACTERIZATION*

Y. Hwang†, T. Tajima, University of California, Irvine, CA USA 92697
G. Anderson, D. J. Gibson, R. A. Marsh, C. P. J. Barty,
Lawrence Livermore National Laboratory, Livermore, CA USA 94550

Abstract

Laser-Compton X-rays have been produced at LLNL, and results agree very well with modeling predictions. An X-ray CCD camera and image plates were calibrated and used to characterize the 30 keV X-ray beam. A resolution test pattern was imaged to measure the source size. K-edge absorption images using thin foils confirm the narrow bandwidth of the source and offer electron beam diagnostics.

INTRODUCTION

X-ray and γ-ray generation by laser-Compton scattering (LCS) is being studied worldwide for its potential as a compact synchrotron quality X-ray source [1–5]. At LLNL, an X-band linac has been built and is in operation to produce laser-Compton scattered X-rays [6]. The output X-ray photons must be well-characterized in many aspects, including the total flux, spectrum and source size. These data are critical not only for knowing the current state of the machine, but also for improving the output by studying their correlation with the electron beam and interaction laser parameters.

MODELING OF X-RAY PHOTONS

All modeling of Compton-scattered X-rays was done with a Mathematica code developed by S. Wu, F. Hartemann, P.C. Yeh and Y. Hwang. The code takes PARMELA outputs from the linac modeling as input electrons, then calculates the Compton cross-section for a laser photon interacting with a PARMELA macroparticle.

When used for imaging simulation, intensity values corresponding to each pixel position are recorded, accounting for any attenuation due to objects in the beam path. Electron-laser overlap for each macroparticle is calculated assuming a ballistic trajectory for the macroparticle and a Gaussian laser beam profile. The pixel intensity values for each macroparticle weighted by the particle's overlap is added incoherently to produce the final image. Figure 1 shows a false-color image simulation of 25 keV X-ray intensity through the 2 mm fused silica back-thinned optic in the beam path, which is used to direct the interaction laser beam head-on with the electron beam.

An analytic method is used to find the photon spectrum within a viewing cone angle [7]. This code uses a simplified form of the cross-section assuming unpolarized laser, and calculates the number of photons at at a given energy within the defined cone. By scanning along an energy range, the spectrum can be plotted with desired precision. Figure 2 shows the energy-angle correlation of Compton scattered photons, with highest energy photons are directed along the electron beam direction.

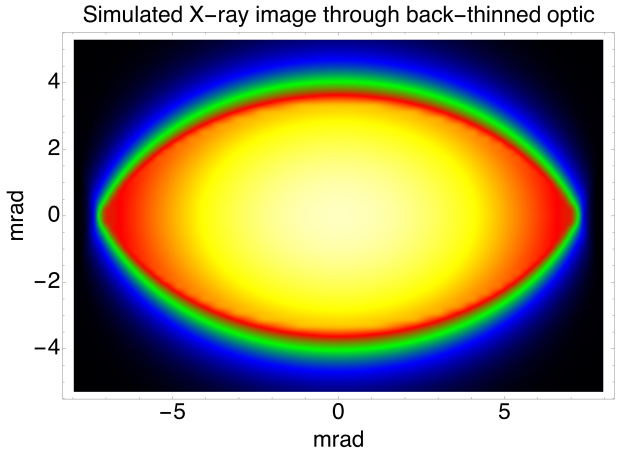

Figure 1: Simulation of an X-ray image.

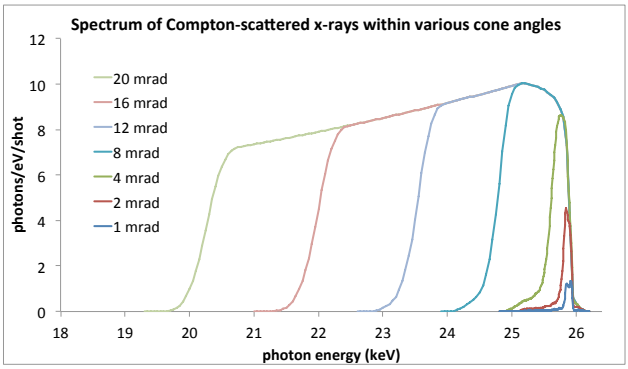

Figure 2: Simulation of X-ray spectra.

FLUX MEASUREMENT

The X-ray flux was measured by counting the calibrated CCD pixel counts within a region. The data was compared with expected flux from simulations.

Camera Calibration

For X-ray detection, an Andor ICCD camera coupled with a scintillator screen via a fiber taper was used. A Beryllium window is fitted at the front to block low energy photons. Two types of scintillators have been used; CsI(Tl) has higher spatial resolution and Gd_2O_2S:Tb (also known as P43) has higher sensitivity. Since scintillator light yield is roughly proportional to the absorbed ionizing energy, the number of

* This work performed under the auspices of the U.S. Department of Energy by Lawrence Livermore National Laboratory under Contract DE-AC52-07NA27344. LLNL-CONF-691080.
† yoonwooh@uci.edu

incident photons can be calculated by taking into account the absorption ratio through the scintillator material, which is dependent on the incident X-ray energy. An important issue is the nonlinearity of scintillator yield as a function of absorbed energy, especially near the K-edges of the scintillator material [8]. Cesium, Iodine and Gadolinium have K-edges at 36.0 keV, 33.2 keV and 50.2 keV respectively. The presence of the K-edges is a challenge for calibrating the camera and thus measuring flux near those energies as the light yield can deviate significantly from absorbed energy and is difficult to predict the discrepancy in different scintillator geometries. Theoretical scintillator-Be window system response spectra assuming a linear light yield is plotted on Fig. 3.

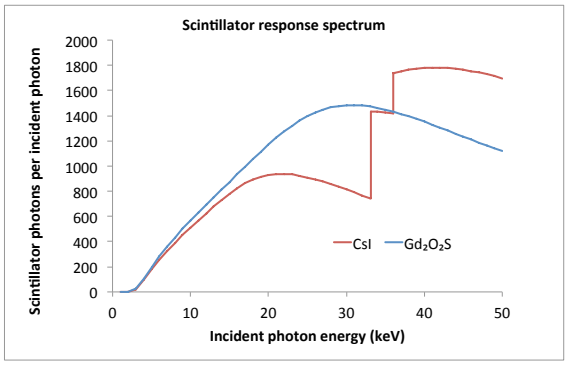

Figure 3: Theoretical scintillator response spectrum assuming linear light yield.

The camera was calibrated using a sealed source of known activity. ^{129}I was chosen for the radioactive source since its emission is mostly in the 30-40 keV range, close to the energy of the Compton-scattered X-rays. because it contains emission above the K-edges of Cesium and Iodine, calibration of CsI with this source is not ideal, but it was the only source at hand with enough activity to reliably measure the signal over background. The CCD is thermoelectrically cooled to -20°C, but it slowly heats up once it reaches minimum temperature and the background counts increase generally linearly for about an hour before fluctuating wildly.

Due to the presence of the Beryllium window, it is very difficult to directly measure with required accuracy the distance between the scintillator and the source, which is critical in determining the solid angle subtended by the imaging area from the source. However, known solid angle versus distance curve can be fitted if enough data exists at different distances that are known relative to each other. The parameters for the fit are the offset distance and magnitude, and the latter is related to the calibration factor we seek. The source was mounted on a translation stage and the intensity was recorded at every 2 mm intervals for at least 15 data points each for forward and backward scan. An example of data and fitted line is shown in Fig. 4. Background counts were subtracted by linearly fitting the background as a function of time and subtracting the amount according to the data file timestamps. Only the central 20 mm radius disk of the image was used in the calculation of intensity to be able to use the disk-to-disk solid angle for various geometry tabulated by Gardner and Verghese [9]. Strong signal and accurate background subtraction are important for this method to be effective. The results showed good agreement between backward and forward scans for CsI calibration but a 15% discrepancy for Gd_2O_2S calibration most likely due to inadequate background characterization. The two values for each scan were averaged and used for the final calibration number: 29.8 keV of absorbed energy per CCD count for CsI and 107 keV/ct for Gd_2O_2S.

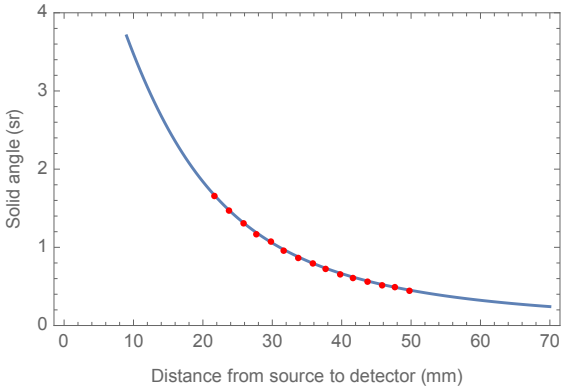

Figure 4: Solid angle best fit as a function of distance.

Flux Measurement

To determine the total flux and compare with simulations, background-subtracted CCD counts for pixels within a 4 mrad cone in the center of the beam image were added up and compared with the expected CCD count based on the simulated spectrum, accounted for the attenuation through the optics and absorption in the scintillator. Total flux is then inferred by the simulated total flux multiplied by the ratio of actual CCD counts to predicted CCD counts. Several simulation parameters such as electron charge and energy were adjusted to match the available data when calculating the flux ratio.

Angular misalignment of the beams and jitters in laser energy/charge can easily reduce the flux by a factor of two or more, especially since the laser beam is extremely long (6 ns) compared to the electron bunch length (3 ps). Nevertheless, the brightest of 1 s exposure (10 shot integration) images have matched the expected flux.

K-EDGE FILTERING

LCS X-rays, due to the Doppler-shifted nature, show energy-angle correlation with highest energy in the direction of the electron beam and decreasing as the deviation increases. By placing a thin foil of material whose K-edge is slightly below the peak energy of the X-rays, an absorption hole in the center of the beam can be observed, and its slope in the lineout profile is directly related to the bandwidth of the beam. Figure 5 shows the experiment and simulated image of a hole created by a 50 µm Silver foil in the beam.

Energy distribution and angular distribution of the electron beam blurs the edge to a gradual slope, as seen in Fig. 6.

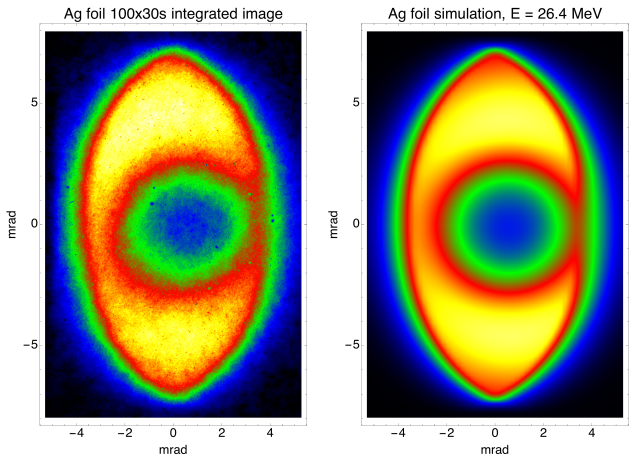

Figure 5: 3000 second integration of Ag foil K-edge image and simulation.

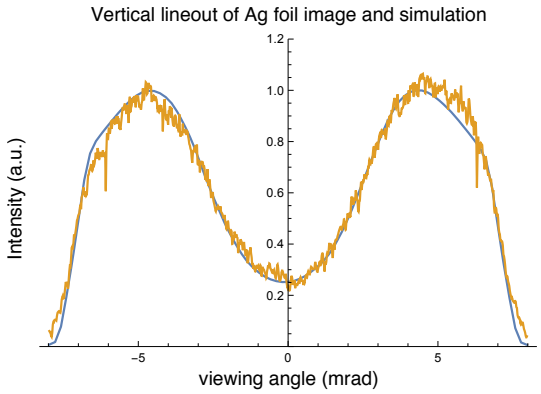

Figure 6: Vertical lineouts of Fig. 5, data (yellow) and simulation (blue).

The shape of the lineout is very sensitive to electron beam parameters. The width is determined by the mean energy and divergence, while the energy spread and divergence contribute to smoothen the slope. If the divergence and energy distribution for a single shot is known, the jitter values can be inferred from the lineout of the integrated image as well. The foil K-edge image is thus a simple yet powerful diagnostic tool for the electron beam.

SPATIAL RESOLUTION AND SOURCE SIZE

The source size of the X-ray should be similar to the size of the electron spot size, since the electron spot size is smaller than the laser spot size at the interaction. OTR measurement of the electron spot size is 10 µm. In order to directly measure the X-ray source size, a high resolution test target and imaging device is necessary. The current CCD camera suffers from blurs due to scintillator thickness and fiber optic mismatch, and is impractical in imaging sub-100 µm details. Knife-edge resolution tests of the two scintillators yielded FWHM resolution of 350 µm for CsI and 700 µm for Gd_2O_2S. We are looking into imaging units that incorporate very thin scintillators and small pixel CCDs for a resolution of 10 µm or better. In the meantime, we have used image plates that have superior spatial resolution to try to measure the upper limit of the source size.

To measure the resolution of the image plate, a knife-edge measurement and a resolution test pattern has been used. A fit of superposition of Gaussian and Cauchy distribution to the slant-edge knife edge image yielded 100 µm FWHM resolution (Fig. 7), while a resolution test pattern placed directly in front of the image plate shows distinguishable line pairs of up to 6 lp/mm (Fig. 8, left). After determining the image plate resolution, the test pattern and the image plate was separated as far as possible to give maximum magnification of about 7x (Fig. 8, right). Low signal-to-noise ratio at the far distance limited the resolution, but it is seen that the source is smaller than 10 lp/mm.

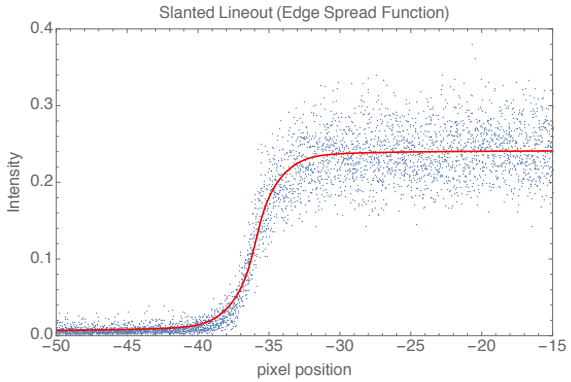

Figure 7: Image plate edge spread function and fit.

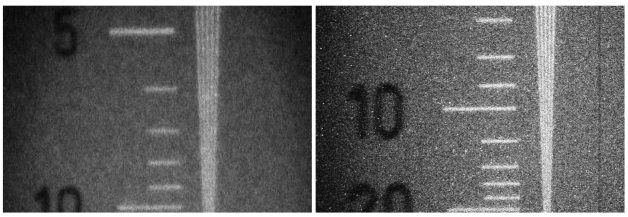

Figure 8: Image plate resolution (left) and source size measurement at 7x magnification (right).

CONCLUSION

We have successfully produced laser-Compton X-rays that match the predicted values in flux and bandwidth based on simulations. Thin foil K-edge profile analysis can be used to characterize the electron beam. Resolution tests confirm the source size smaller than what we can resolve; a better imaging solution is being sought.

REFERENCES

[1] I. V. Pogorelsky *et al.*, "Demonstration of 8 × 10^{18}photons/second peaked at 1.8 Å in a relativistic Thomson scattering experiment", *Phys. Rev. ST Accel. Beams*, vol. 3, p. 090702, 2000.

[2] R. Kuroda *et al.*, "Quasi-monochromatic hard X-ray source via laser Compton scattering and its application", *Nucl. Instr. Meth. A*, vol. 637, pp. S183-S186, 2011.

[3] Y. Du *et al.*, "Generation of first hard X-ray pulse at Tsinghua Thomson Scattering X-ray Source", *Rev. Sci. Instr.*, vol. 84, p. 053301, 2013.

[4] Y. K. Wu, in *Proc. IPAC'10*, pp. 2648–2650.

[5] R. J. Loewen, "A compact light source: Design and technical feasibility study of a laser-electron storage ring X-ray source", Stanford Linear Accelerator Center, Stanford University, Stanford, CA, USA, 2003

[6] D. J. Gibson *et al.*, in *Proc. IPAC'15*, pp. 1363–1365.

[7] J. Wang and W. Huang, "Spectral distributions of the scattered photons within an acceptance angle in Thomson scattering", *Chin. Phys. C*, vol. 35, no. 2, pp. 203-208, 2011.

[8] W. Mengesha, T. D. Taulbee, B .D. Rooney, and J. D. Valentine, "Light Yield Nonproportionality of CsI(Tl), CsI(Na), and YAP", *IEEE Trans. Nucl. Sci.*, vol. 45, no. 3, pp. 456-461, 1998.

[9] R. P. Gardner and K. Verghese, "On the solid angle subtended by a circular disc", *Nucl. Instr. Meth.*, vol. 93, no. 1, pp. 163-167, 1971.